

Adapprox: Adaptive Approximation in Adam Optimization via Randomized Low-Rank Matrices

Pengxiang Zhao¹ Ping Li² Yingjie Gu² Yi Zheng² Stephan Ludger Kölker² Zhefeng Wang²
Xiaoming Yuan¹

Abstract

As deep learning models exponentially increase in size, optimizers such as Adam encounter significant memory consumption challenges due to the storage of first and second moment data. Current memory-efficient methods like Adafactor and CAME often compromise accuracy with their matrix factorization techniques. Addressing this, we introduce Adapprox, a novel approach that employs randomized low-rank matrix approximation for a more effective and accurate approximation of Adam’s second moment. Adapprox features an adaptive rank selection mechanism, finely balancing accuracy and memory efficiency, and includes an optional cosine similarity guidance strategy to enhance stability and expedite convergence. In GPT-2 training and downstream tasks, Adapprox surpasses AdamW by achieving 34.5% to 49.9% and 33.8% to 49.9% memory savings for the 117M and 345M models, respectively, with the first moment enabled, and further increases these savings without the first moment. Besides, it enhances convergence speed and improves downstream task performance relative to its counterparts.

1. Introduction

In the field of deep learning, optimization algorithms play a pivotal role in training models both efficiently and effectively. Among the most popular optimization algorithms is the Adam (Kingma & Ba, 2014), and its variant, AdamW (Loshchilov & Hutter, 2018), known for their robust performance across diverse applications. However, the shift from smaller architectures like AlexNet (Krizhevsky et al.,

Work was done when Pengxiang Zhao was an intern at Huawei Cloud System AI innovation Lab. ¹Department of Mathematics, The University of Hong Kong, Hong Kong, China ²System AI Innovation Lab, Huawei Cloud, Hangzhou, China. Correspondence to: Xiaoming Yuan <xmyuan@hku.hk>.

Preprint. Work in Progress

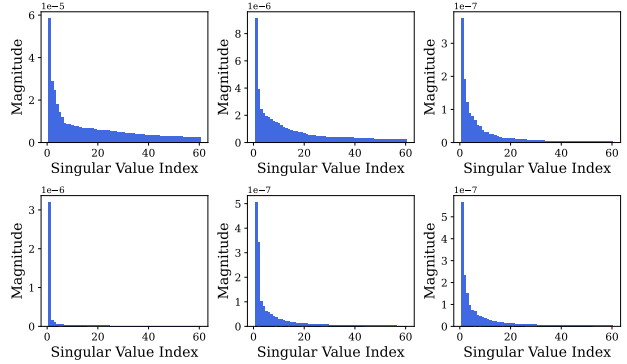


Figure 1. Singular value distributions. This figure shows the top 60 singular values from six second moment matrices, out of a full rank of 1,024, obtained from AdamW training a GPT-2 345M model at the 45,000th iteration.

2017) with fewer than 100 million parameters, to colossal models such as GPT-3 (Brown et al., 2020), encompassing over 100 billion parameters, poses substantial memory consumption challenges. This issue becomes particularly acute in resource-constrained environments (Steiner et al., 2023). Despite its effectiveness, the Adam optimizer exacerbates this challenge by necessitating significant memory to store both first and second moments for each parameter to maintain adaptive learning rates.

There have been notable efforts in the development of memory-efficient optimizers (Shazeer & Stern, 2018; Anil et al., 2019; Li et al., 2023; Luo et al., 2023). Adafactor (Shazeer & Stern, 2018) offers the option to omit Adam’s first moment, while utilizing a factored representation for the second moment. However, Adafactor tends to show a decrease in training effectiveness, which is primarily linked to the unavoidable approximation errors that occur in its matrix factorization approach (Anil et al., 2019; Luo et al., 2023). To mitigate this performance degradation and improve training stability, the CAME optimizer (Luo et al., 2023) extends Adafactor with a confidence-based scaling factor for the parameter updates. Nevertheless, CAME still relies on the same fundamental factorization technique to

store the second moment and confidence statistics, thus inheriting the core challenges encountered by Adafactor.

In this study, we present Adapprox, a novel approach designed to overcome the limitations associated with memory-efficient optimizers that rely on matrix factorization. Our work is motivated by a crucial observation: in many large-scale model training scenarios, the second moment matrices often have a limited number of dominant singular values, with the rest exhibiting substantially lower magnitudes. This insight is corroborated by empirical evidence, illustrated in Figure 1. Consequently, Adapprox employs randomized low-rank matrix approximation (Liberty et al., 2007; Li et al., 2014; Batselier et al., 2018) to effectively approximate the second moment in Adam. Our method primarily reduces memory usage by distilling key features from large matrices, while also ensuring a more precise representation.

Figure 1 also elucidates the limitations of fixed 1-rank approximations used in Adafactor and CAME. This approach’s tendency to compromise accuracy due to multiple dominant singular values is evident in the top row of plots in Figure 1. However, in these instances, a modest increase in the target rank for approximation can substantially improve accuracy. Considering the singular value distribution patterns of the second moment, as illustrated in Figure 1, overestimating the target rank in low-rank approximations can lead to computationally intensive processes with minimal precision improvements. Conversely, underestimating the rank significantly compromises accuracy. In response to this, Adapprox introduces a dynamic rank-selection mechanism, designed to adaptively select an optimal rank for each target matrix within the low-rank approximation process.

Furthermore, to mitigate systematic errors inherent in low-rank approximations, our approach optionally integrates a cosine similarity guidance mechanism. This method computes the cosine similarity between each update and the first moment, subsequently adjusting the learning rate for that step proportionally. A low cosine similarity results in a reduced update, while a high similarity prompts an increase in the update magnitude.

We evaluated our method through the pretraining of GPT-2 across various configurations and associated downstream tasks. The findings demonstrate that our approach achieves reduced memory usage compared to Adam, while maintaining only a marginally higher memory footprint than Adafactor and CAME. Crucially, our method not only maintains performance on par with Adam but also enables accelerated convergence and improved generalization performance.

Our study’s key contributions are as follows:

- In light of the singular value distribution of the second moment in Adam, we present Adapprox, which utilizes randomized low-rank matrix approximation to

effectively approximate the second moment in Adam.

- We develop an adaptive rank selection mechanism that balances precision and memory savings by choosing an appropriate rank for approximating the target matrix.
- We integrate an optional cosine similarity guidance strategy into Adapprox, which aims to expedite the convergence process and enhance the stability.
- We showcase Adapprox’s efficacy on the GPT-2 pre-training and several downstream tasks. Enabling the first moment, Adapprox achieves memory savings ranging from 34.5% to 49.9% for the GPT-2 117M model and 33.8% to 49.9% for the 345M model, compared to AdamW. Disabling the first moment elevates these savings to 84.5% to 99.9% for the 117M model, and to 83.8% to 99.9% for the 345M model. Furthermore, our experimental results suggest that Adapprox may offer faster convergence and potentially improved performance outcomes.

2. Related Work

Memory Efficient Optimizers. Memory efficient optimizers aim to reduce memory usage by compressing optimizer states during training, ideally without affecting the performance efficacy of their standard counterparts. Adafactor (Shazeer & Stern, 2018) reduces memory usage by employing two main strategies: the first is the optional omission of Adam’s first moment; and the second is the compression of the second moment using a novel 1-rank matrix factorization approach based on minimizing I-divergence (Lee & Seung, 1999). While Adafactor achieves notable memory savings and computational efficiency, it is crucial to recognize the potential compromise in accuracy that may arise from its factorization approach (Anil et al., 2019; Luo et al., 2023). SM3 (Anil et al., 2019) represents a memory efficient variation of Adagrad (Duchi et al., 2011). Experimentally, it proves especially effective in situations where gradients show natural activation patterns. CAME (Luo et al., 2023) builds upon Adafactor’s framework by incorporating a confidence-guided strategy to elevate approximation accuracy. However, this method also involves compressing and storing confidence data using an identical matrix factorization technique, resulting in similar accuracy-related challenges. Moreover, CAME’s dependency on the first moment for its confidence strategy limits the potential for omitting this data, thereby constraining further memory savings. 4-bit Adam (Li et al., 2023) employs quantization techniques to compress Adam’s first and second moments. Notably, this quantization is compatible with matrix factorization methods.

Low-Rank Matrix Approximation. Low-rank matrix approximation seeks to represent a matrix using lower-rank

matrices, aiming for a more efficient data representation while endeavoring to retain as much information as possible. Low-rank matrix approximation is utilized across a wide spectrum of applications, including principal component analysis (PCA) (Shen & Huang, 2008; Papailiopoulos et al., 2013), image processing (Haeffele et al., 2014; Guo et al., 2017; Chen et al., 2017), and a variety of machine learning scenarios (Paterek, 2007; Li et al., 2016).

3. Methodology

This section begins with a brief overview of Adam, followed by an examination of the randomized low-rank approximation method. Subsequently, we introduce the adaptive rank selection mechanism. We then provide a comprehensive description of the Adapprox optimizer. Lastly, we delve into the proposed cosine similarity guidance strategy.

3.1. Overview of the Adam Optimizer

Consider a function $f(W)$, where $W \in \mathbb{R}^{m \times n}$ denotes the parameters of the neural network. The update rule for Adam (Kingma & Ba, 2014) at the t -th iteration is defined as follows:

$$(\text{Adam}) \begin{cases} G_t &= \nabla f(W_{t-1}), \\ M_t &= \beta_1 M_{t-1} + (1 - \beta_1) G_t, \\ V_t &= \beta_2 V_{t-1} + (1 - \beta_2) G_t^2, \\ \hat{M}_t &= M_t / (1 - \beta_1^t), \\ \hat{V}_t &= V_t / (1 - \beta_2^t), \\ W_t &= W_{t-1} - \alpha \hat{M}_t / (\sqrt{\hat{V}_t} + \epsilon). \end{cases} \quad (1)$$

Here, all computations are element-wise. G_t represents the gradient arranged in matrix form. M_t and V_t are the exponential running averages of the first and second moments, respectively. \hat{M}_t and \hat{V}_t are the bias-corrected versions of M_t and V_t . β_1 and β_2 control these moment estimates. Additionally, α denotes the learning rate, and ϵ is a small positive constant introduced to prevent division by zero.

Building upon Adam, AdamW (Loshchilov & Hutter, 2018) decouples weight decay from the gradient updates. With this change, the parameter update step in AdamW is

$$W_t = W_{t-1} - \alpha(\hat{M}_t / (\sqrt{\hat{V}_t} + \epsilon) + \lambda W_{t-1}), \quad (2)$$

where λ is the rate of the weight decay.

As mentioned, Adam requires the storage of both M_t and V_t at each step, which requires $O(mn)$ extra memory.

3.2. Low-Rank Approximation of the Second Moment

For a matrix $A \in \mathbb{R}^{m \times n}$, deriving its low-rank approximation can be formulated as an optimization problem:

$$\min_{Q, U} \|A - QU^\top\|_F^2, \quad (3)$$

where $\|\cdot\|_F$ is the Frobenius norm and $Q \in \mathbb{R}^{m \times k}$ and $U \in \mathbb{R}^{n \times k}$ are two feature matrices ($1 \leq k \ll \min\{m, n\}$). Then, $A_k = QU^\top$ is the k -rank approximation of A . The optimal A_k can be determined by performing a full Singular Value Decomposition (SVD) and then truncating it to retain only the top k singular values and their corresponding singular vectors, resulting in the following representation (see Theorem 2.4.8 in (Golub & Van Loan, 2013)):

$$A_k = \sum_{i=1}^k \sigma_i u_i v_i^\top, \quad (4)$$

where $\sigma_1 \geq \sigma_2 \geq \dots \geq \sigma_k \geq 0$ are the top k singular values of A , and u_i and v_i ($1 \leq i \leq k$) are corresponding left and right singular vectors. The approximation error can be explicitly expressed as follows:

$$\|A - A_k\|_F^2 = \sum_{i=k+1}^{\min\{m, n\}} \sigma_i^2. \quad (5)$$

Given Equation (5) and the singular value distribution of the second moment matrix shown in Figure 1, utilizing a k -rank approximation to compress the second moment matrix emerges as a rational choice. Nevertheless, the computation of the full SVD for large matrices presents considerable computational and memory challenges. We mitigate these issues by leveraging randomized low-rank matrix approximation algorithms (Liberty et al., 2007; Halko et al., 2011; Nakatsukasa, 2020), which provide a balance of computational efficiency and memory economy, while still delivering high-quality low-rank approximations.

Our implementation utilizes the Gaussian sampling variant of the randomized SVD algorithm (Halko et al., 2011). In our approach, we bypass the SVD estimation to streamline the process, concentrating solely on the extraction of feature matrices without the need for singular values. Additionally, we incorporate an oversampling mechanism, which further refines the algorithm's ability to capture more precise subspace representations. The comprehensive procedure of this modified method is detailed in Algorithm 1, termed Streamlined Randomized Subspace Iteration (S-RSI).

The S-RSI aims to compute an approximate basis $Q \in \mathbb{R}^{m \times k}$ which has orthonormal columns for the column space of the target matrix $A \in \mathbb{R}^{m \times n}$ such that

$$A_k = QQ^\top A. \quad (6)$$

We form $U = Q^\top A$, and thus we obtain two feature matrices $Q \in \mathbb{R}^{m \times k}$ and $U^\top \in \mathbb{R}^{n \times k}$. Computing Q is highly efficient using random sampling methods. Consider drawing a random vector u , with each element independently and identically distributed according to a standard Gaussian distribution. When we compute $q = Au$, it effectively

Algorithm 1 Streamlined Randomized Subspace Iteration

Inputs: Target matrix $A \in \mathbb{R}^{m \times n}$, target rank k , integer l , and integer p with $(k + p) \leq \min\{m, n\}$
 $U \sim \mathcal{N}(0, 1)$
 $Q, R \leftarrow \mathbf{0}^{m \times (k+p)}, \mathbf{0}^{(k+p) \times (k+p)}$
for $i \leftarrow 1, 2, \dots, l$ **do**
 $Q \leftarrow AU$
 $Q, R \leftarrow \text{QR decomposition}(Q)$
 $U \leftarrow A^\top Q$
end for
return $Q[:, :k], U^\top[:, :k]$

serves as a stochastic representation of the column space of A , because q represents a random linear combination of the columns of A . By repeating this sampling process k times, we get a set of random vectors:

$$\{q_i \mid q_i = Au_i, i = 1, 2, \dots, k\}. \quad (7)$$

Due to the inherent randomness in u_i 's generation, the set of vectors $\{u_i\}_{i=1}^k$ are expected to occupy a general linear position, which implies a high likelihood that any subset of these vectors is linearly independent. Consequently, this observation leads us to propose the following:

Proposition 3.1. *Given a set of randomly generated vectors $\{u_i\}_{i=1}^k$ that are in a general linear position, and a full rank matrix $A \in \mathbb{R}^{m \times n}$, the set of vectors $\{q_i \mid q_i = Au_i\}_{i=1}^k$ are also linearly independent.*

Proof. Linear independence of $\{u_i\}_{i=1}^k$ implies that $\sum_{i=1}^k a_i u_i = 0$ holds when all scalars $\{a_i\}_{i=1}^k$ are zero. We examine a linear combination of the vectors $\{q_i\}_{i=1}^k$:

$$\sum_{i=1}^k a_i q_i = \sum_{i=1}^k a_i Au_i = A \sum_{i=1}^k a_i u_i. \quad (8)$$

As A is full rank, $\sum_{i=1}^k a_i q_i \neq 0$ unless all a_i are zero, indicating that vectors $\{q_i\}_{i=1}^k$ are linearly independent. \square

Consequently, to derive an orthonormal basis for the column space of matrix A , we first arrange the set $\{q_i\}_{i=1}^k$ as the columns of a matrix Q , and then we apply an orthonormalization procedure, like QR decomposition (Golub & Van Loan, 2013).

To enhance the precision of random sampling for basis determination in scenarios where the input matrix exhibits a flat singular spectrum and is of considerable size, we incorporate a power iteration technique (Rokhlin et al., 2010; Halko et al., 2011; Golub & Van Loan, 2013). Specifically, this approach applies the randomized sampling methodology to the modified matrix

$$A' = (AA^\top)^l A, \quad (9)$$

where l is a small integer (for example, $l = 5$). According to SVD, matrix A can be expressed as $A = Q\Sigma U^\top$, where Q and U are orthogonal matrices encapsulating the left and right singular vectors of A , respectively, and Σ is a diagonal matrix composed of the singular values of A . Then, A' is derived as follows:

$$A' = (Q\Sigma U^\top U\Sigma Q^\top)^l Q\Sigma U^\top = Q(\Sigma)^{2l+1} U^\top. \quad (10)$$

Hence, while A' retains the same singular vectors as A , its singular values exhibit an accelerated rate of decay:

$$\sigma_i(A') = \sigma_i(A)^{2l+1}, \quad (11)$$

This enhances the efficacy of distinguishing between more significant and less significant singular vectors, thereby improving the overall accuracy of the approximation. Furthermore, to augment the precision, we utilize a small oversampling parameter p , such as $p = 5$, to increase the sample size beyond the target rank, thereby providing a buffer that mitigates the risk of omitting significant components.

Through the S-RSI method, we can efficiently compress the storage of matrix A from $O(mn)$ to $O(k(m+n))$ by retaining only matrices Q and U^\top with time complexity of $O(lmn(k+p))$. Following the randomized SVD algorithm (Halko et al., 2011), the approximation error bound is:

$$\mathbb{E}\|A - QU^\top\| \leq \left[\left(1 + \sqrt{\frac{k}{p-1}} \right)^{2l+1} \sigma_{k+1}^{2l+1} + \frac{e\sqrt{k+p}}{p} \sqrt{\sum_{j>k} \sigma_j^{2(2l+1)}} \right]^{1/(2l+1)}. \quad (12)$$

According to Equation (12), the approximation error can be reduced by increasing not just k , but also p and l . We further demonstrate the efficacy of the S-RSI through empirical comparisons. Specifically, we evaluate its performance in comparison to Adafactor's matrix factorization approach and the SVD, focusing on all second-moment matrices obtained during the training of a GPT-2 345M model using AdamW. Results are shown in Figure 2.

Figure 2 compares the mean approximation error and computation time of varying ranks, with the S-RSI employing hyperparameters $l = 5$ and $p = 5$. Adafactor's factorization method employs a fixed 1-rank approximation, leading to consistent results regardless of rank changes. The SVD serves as a benchmark for optimal low-rank approximation. The SVD and S-RSI show a substantial decrease in approximation error with a minimal increase in rank. Besides, as the rank increases, the S-RSI approaches the SVD benchmark. In terms of computation time, Adafactor is the most efficient with a consistent duration. The S-RSI not only significantly reduces computation time compared to SVD

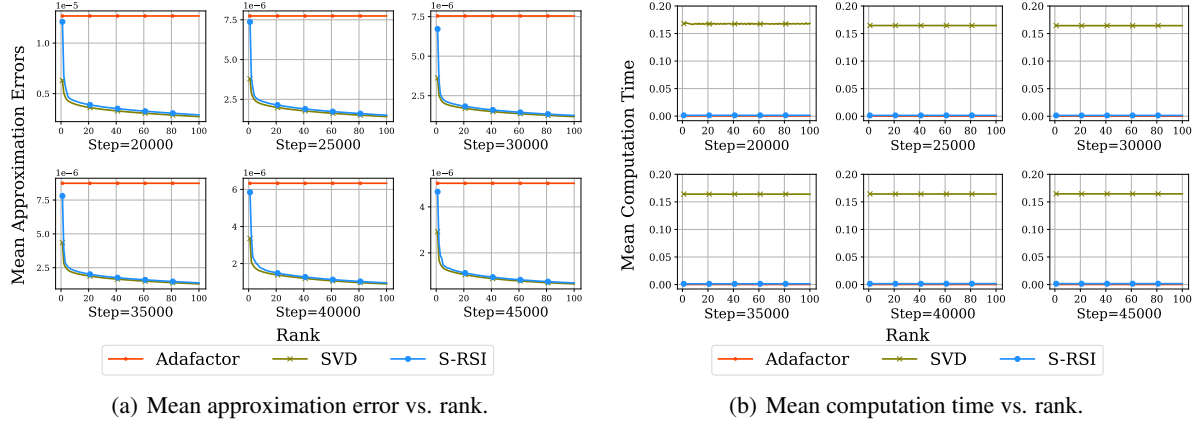


Figure 2. Comparative analysis of the S-RSI ($l = 5$ and $p = 5$) against Adafactor and SVD. All methods are applied to the second-moment matrices derived from training a GPT-2 345M model using the AdamW, with results captured at various stages of the training process.

but also approaches the efficiency of Adafactor. While the S-RSI shows a linear relationship with rank k theoretically, the actual rate of increase is considerably less than k . This can be largely attributed to the multi-core architecture of GPUs and parallel computing. Consequently, the S-RSI provides an advantageous balance of approximation accuracy and computational efficiency.

3.3. Adaptive Rank Selection

The results in Figure 2 underscore the importance of selecting the proper rank k for the S-RSI. Choosing a larger k can result in increased computational demands for minimal precision improvements, while a smaller k risks significantly compromising accuracy. To address this, we develop an adaptive rank selection mechanism, which dynamically adjusts k for each target matrix.

The algorithm updates the rank k_t at regular intervals of Δs steps. Initially set as k_{init} , k_t is used to perform the S-RSI. Then, we evaluate the approximation error rate:

$$\xi = \frac{\|A - QU^\top\|_F}{\|A\|_F}. \quad (13)$$

Should ξ rise above a threshold ξ_{thresh} , k_t is adjusted to $k_t + f(\xi)$, ensuring that it does not exceed the maximum rank k_{max} . We model f as a variant of the sigmoid function including four hyperparameters η, ω, ϕ and τ :

$$f(\xi) = \left\lfloor \frac{\eta}{\exp(\omega\xi + \phi) + \tau} \right\rfloor, \quad \xi > 0, \quad (14)$$

where $\eta > 0$ sets the upper bound of f 's range, $\omega < 0$ dictates the rate of change, and ϕ and τ adjust the function's offset. This adheres to the heuristic principle that as ξ increases, the expansion rate of k_t should initially be gradual, then accelerate, and ultimately stabilize near an upper limit.

Algorithm 2 Adaptive S-RSI

Inputs: Target matrix $A \in \mathbb{R}^{m \times n}$, rank k_{t-1} , initial rank k_{init} , the maximum rank k_{max} , integer l , integer p , threshold ξ_{thresh} , step t , and adaptive interval Δs

if $(t \bmod \Delta s) = 1$ **then**

$k_t \leftarrow k_{init}$

repeat

$Q, U^\top \leftarrow \text{S-RSI}(A, k_t, l, p)$

$\xi \leftarrow \|A - QU^\top\|_F / \|A\|_F$

$k_t \leftarrow \min\{k_t + f(\xi), k_{max}\}$ {Equation (14)}

$p \leftarrow \min\{p, k_{max} - k_t\}$

until $\xi \leq \xi_{thresh}$

else

$k_t \leftarrow k_{t-1}$

$Q, U^\top \leftarrow \text{S-RSI}(A, k_t, l, p)$

end if

return $Q[:, :k_t], U^\top[:, :k_t], k_t$

By Equation (7), this extension requires sampling $f(\xi)$ additional vectors from a standard Gaussian distribution and then applying QR decomposition again. The revised k_t is then maintained for the next Δs iterations. The pseudocode for this method is summarized in Algorithm 2, which we designate as Adaptive S-RSI (AS-RSI).

3.4. Adapprox Algorithm

The integration of the proposed methodologies culminates in the Adapprox algorithm defined in Algorithm 3. At each step, f_t represents a stochastic realization of the objective function f , exemplified by the loss function computed using a randomly selected mini-batch of data. We then compute the gradient G_t relative to the previous parameters and the exponential running averages of the second moment V_t . Note that V_{t-1} is reconstructed from $Q_{t-1}U_{t-1}^\top$, while V_t

Algorithm 3 Adapprox

Inputs: Initial point $W_0 \in \mathbb{R}^{m \times n}$, $M_0 = \mathbf{0}^{m \times n}$ and $V_0 = \mathbf{0}^{m \times n}$, learning rates $\{\alpha_t\}_{t=1}^T$, moment decay β_1 and β_2 , small constant ϵ , clipping threshold d , initial rank k_{init} , the maximum rank k_{max} , integer l , integer p with $(k_{init} + p) \leq k_{max}$, threshold ξ_{thresh} , adaptive interval Δs , and weight decay rate λ
 Initialize $Q_0 = \mathbf{0}^{m \times k_{init}}$, $U_0^\top = \mathbf{0}^{n \times k_{init}}$, $k_0 = k_{init}$
for $t \leftarrow 1, 2, \dots, T$ **do**
 $G_t \leftarrow \nabla f_t(W_{t-1})$
 $V_t \leftarrow \beta_2 Q_{t-1} U_{t-1}^\top + (1 - \beta_2) G_t^2$
 $Q_t, U_t^\top, k_t \leftarrow \text{AS-RSI}(V_t, k_{t-1}, k_{init}, k_{max}, l, p, \xi_{thresh}, t, \Delta s)$
 $M_t \leftarrow G_t / (\sqrt{V_t} + \epsilon)$
 $M_t \leftarrow M_t / \max(1, \text{RMS}(M_t)/d)$
 if $\beta_1 > 0$ **then**
 $M_t \leftarrow \beta_1 M_{t-1} + (1 - \beta_1) M_t$
 end if
 $W_t \leftarrow W_{t-1} - \alpha_t (M_t + \lambda W_{t-1})$
end for

is factored using the AS-RSI. Subsequently, we calculate the update $M_t = G_t / (\sqrt{V_t} + \epsilon)$ and incorporate the update clipping mechanism as proposed in (Shazeer & Stern, 2018) to mitigate excessively large updates:

$$M_t \leftarrow \frac{M_t}{\max(1, \text{RMS}(M_t)/d)}, \quad \text{RMS}(M_t) = \frac{\|M_t\|_F}{\sqrt{mn}},$$

where d is the clipping threshold. We also offer the option to omit the first moment, depending on whether β_1 is set to zero. Finally, parameter updates are executed in a decoupled weight decay fashion, as delineated in Equation (2).

The proposed Adapprox, while rooted in Adam, diverges in three key aspects: (1) it omits the bias correction steps; (2) it integrates an update clipping mechanism that enhances performance (as detailed in Appendix A); and (3) it modifies the first moment accumulator, replacing the running average of the gradient with the running average of the update.

3.5. Cosine-Similarity Guidance Strategy

Inspired by CAME, we incorporate an optional mechanism aimed at enhancing the update process and expediting the training phase when $\beta_1 > 0$. Specifically, this involves a heuristic method that utilizes the cosine similarity between the current update and the running average of updates to assess the confidence level of the approximation.

To elaborate, for the given current update

$$\hat{M}_t \leftarrow \frac{G_t}{\sqrt{V_t} + \epsilon}, \quad \hat{M}_t \leftarrow \frac{\hat{M}_t}{\max(1, \text{RMS}(\hat{M}_t)/d)}, \quad (15)$$

and the running average of updates

$$M_t \leftarrow \beta_1 M_{t-1} + (1 - \beta_1) \hat{M}_t, \quad (16)$$

we calculate the cosine similarity measure

$$\theta_{cos} = \frac{\sum_{i,j} (\hat{M}_t \odot M_t)_{ij}}{\|\hat{M}_t\|_F \|M_t\|_F} \in [-1, 1], \quad (17)$$

where \odot denotes element-wise multiplication.

When θ_{cos} approaches 1, it indicates a better alignment between the directions of \hat{M}_t and M_t . Conversely, a θ_{cos} value close to -1 suggests poor alignment. In the case where $\theta_{cos} = 0$, \hat{M}_t and M_t are orthogonal to each other. To modulate the update based on θ_{cos} , we introduce a factor that either penalizes or accelerates the update accordingly:

$$M_t \leftarrow \frac{M_t}{1 - \theta_{cos} + \epsilon}, \quad (18)$$

which adjusts M_t inversely with respect to θ_{cos} , enhancing the update for alignment and penalizing it for divergence.

It is noteworthy that our proposed cosine-similarity guidance strategy is effective exclusively when $\beta_1 > 0$, which is consistent with CAME. However, our strategy is designed to utilize only the information available at the current step, thereby obviating the need for extra memory.

4. Experiments

In this section, we present a comparative analysis of Adapprox against existing counterparts in pretraining GPT-2 (Radford et al., 2019) and in subsequent downstream tasks.

4.1. Setup

We investigate two GPT-2 configurations: 117M and 345M, as outlined in Table 1. Our pretraining experiments utilize The Pile dataset (Gao et al., 2020) and the SentencePiece tokenizer (Kudo & Richardson, 2018). We evaluate the pretrained models on several downstream tasks, including SQuAD v1.1 (Rajpurkar et al., 2016), CoLA (Warstadt et al., 2018), MRPC (Dolan & Brockett, 2005), SST-2 (Socher et al., 2013), and MNLI-m (Williams et al., 2017). Our primary baselines include AdamW (Loshchilov & Hutter, 2018), Adafactor (Shazeer & Stern, 2018), and CAME (Luo et al., 2023). We have implemented our optimization algorithm using the PyTorch framework (Paszke et al., 2019). Additionally, the pretraining of GPT-2 is conducted utilizing the Megatron-LM framework (Shoeybi et al., 2019) and eight NVIDIA Tesla V-100 GPUs.

For GPT-2 pretraining, we set β_1 and β_2 at 0.9 and 0.999, respectively, and maintain a consistent weight decay rate of 0.1 for all compared algorithms. Adapprox’s additional parameters are specified as follows: $\epsilon = 1 \times 10^{-8}$, $d = 1$, $k_{init} = 1$,

Table 1. Model configurations.

| SIZE | LAYERS | HIDDEN | HEADS | SEQUENCE LENGTH |
|------|--------|--------|-------|-----------------|
| 117M | 12 | 768 | 12 | 1024 |
| 345M | 24 | 1024 | 16 | 1024 |

Table 2. Quantitative memory usage (MB) comparison.

| β_1 | METHOD | GPT-2 117M | GPT-2 345M |
|-----------|-------------------------|----------------|-----------------|
| 0.9 | AdamW | 949.7 (100.0%) | 2707.5 (100.0%) |
| | Adafactor | 476.1 (50.1%) | 1356.7 (50.1%) |
| | CAME | 476.8 (50.2%) | 1358.4 (50.2%) |
| | Adapprox (k_{init}) | 476.1 (50.1%) | 1356.7 (50.1%) |
| | Adapprox (k_{max}) | 622.0 (65.5%) | 1791.1 (65.5%) |
| 0.0 | AdamW | 949.7 (100.0%) | 2707.5 (100.0%) |
| | Adafactor | 1.2 (0.1%) | 2.9 (0.1%) |
| | CAME | — | — |
| | Adapprox (k_{init}) | 1.2 (0.1%) | 2.9 (0.1%) |
| | Adapprox (k_{max}) | 147.2 (15.5%) | 437.4 (16.2%) |

$k_{max} = 0.25 \min\{m, n\}$, $l = 5$, $p = 5$, $\xi_{thresh} = 0.01$, $\Delta s = 10$, and $\eta = 200$, $\omega = -10$, $\phi = -2.5$, $\tau = -9$. For Adafactor and CAME, the other parameters are set to their respective default values. We adopt a linear warmup strategy followed by a cosine-style learning rate decay, both integrated within the Megatron-LM framework. To guarantee fair comparisons, all evaluated optimizers use uniform training parameters for each model, selected through empirical testing and established best practices. Specifically, the batch size, number of training iterations, number of warmup iterations, peak learning rate, and minimum learning rate are set as follows: for GPT-2 117M, they are 128, 100K, 1K, 3×10^{-4} , and 5×10^{-5} ; and for GPT-2 345M, 128, 100K, 1K, 3×10^{-4} , and 3×10^{-5} , respectively.

For downstream tasks, we fine-tune GPT-2 models pre-trained with each evaluated optimizer for three epochs, adjusting learning rates individually per task. Besides, cosine-similarity guidance is not employed in the fine-tuning process of Adapprox.

4.2. Memory Usage Comparison

We assess the memory footprint associated with the state of each optimizer. Adapprox utilizes an adaptive low-rank approximation, and we report its memory usage based on predetermined k_{init} and k_{max} values. The actual memory usage falls between these boundaries. The results are listed in Table 2. While Adapprox does increase memory usage compared to Adafactor and CAME, it allows for a flexible trade-off between memory efficiency and accuracy through the adjustment of k_{init} and k_{max} . In comparison to AdamW

and with $\beta_1 = 0.9$, Adapprox achieves memory reductions of 34.5% to 49.9% for GPT-2 117M and 33.8% to 49.9% for GPT-2 345M. With $\beta_1 = 0$, CAME becomes non-viable, while AdamW still allocates memory for the first moment. In contrast, both Adafactor and Adapprox completely forego first moment memory allocation. In such scenarios, Adapprox yields significant memory savings: 84.5% to 99.9% for GPT-2 117M and 83.8% to 99.9% for GPT-2 345M.

4.3. GPT-2 Training

Figure 3 presents the empirical comparison of Adapprox with AdamW, Adafactor, and CAME in the pretraining of GPT-2 models. The top row shows the validation loss across the 117M and 345M GPT-2 models, respectively, from left to right. The bottom row displays the validation perplexity for these models, arranged in the same sequence. Relative to AdamW, Adapprox generally exhibits better validation loss and perplexity on the GPT-2 117M model, while delivering comparable results on the GPT-2 345M. Adafactor consistently underperforms compared to Adapprox, although the performance difference on the GPT-2 345M is relatively modest. While CAME initially shows lower validation loss and perplexity, it tends to converge to suboptimal outcomes over time. These results indicate that Adapprox effectively balances accuracy with memory usage and potentially offers faster convergence and superior performance compared to Adafactor and CAME.

4.4. Downstream Tasks

We evaluate the downstream task performance of GPT-2 110M and 345M models, each pretrained and fine-tuned with its corresponding optimizer. The empirical results are presented in Table 3. Our experimental findings underscore the superiority of Adapprox, as evidenced by better performance of GPT-2 models trained and fine-tuned using it, compared to those using Adafactor and CAME. Besides, Adapprox not only achieves performance comparable to AdamW but also surpasses it in certain tasks. Additionally, we observe that Adapprox exhibits stable performance across various learning rates, a conclusion drawn from employing grid search to determine optimal learning rates for different downstream tasks. In contrast, CAME shows sensitivity to learning rate selection, frequently underperforming relative to other optimizers in these scenarios. For detailed evidence, refer to Appendix B.

5. Discussion

While Adapprox and Adafactor achieve significant memory savings through the low-rank approximation of the second moment and by omitting the first moment (seen in Table 2), our experiments demonstrate that the absence of the first moment has a notable impact on convergence speed and overall

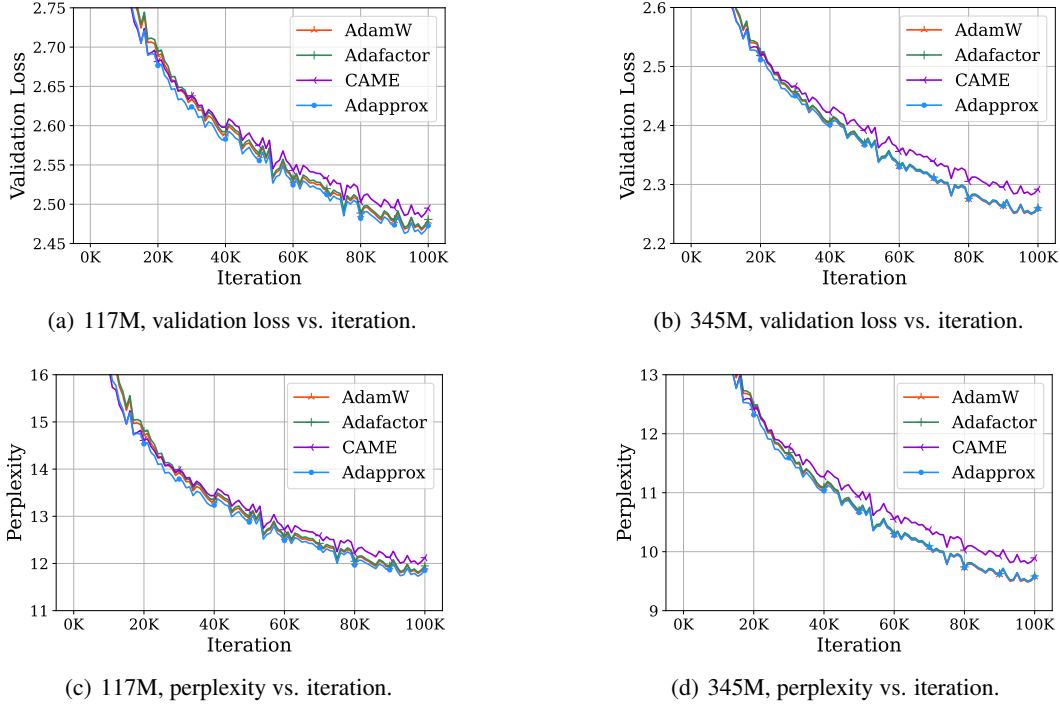


Figure 3. Comparative analysis of Adapprox against AdamW, Adafactor, and CAME on pretraining GPT-2 models.

Table 3. Results of fine-tuning performance on downstream tasks.

| MODEL | METHOD | SQuAD v1.1 (F1) | CoLA (Acc) | MRPC (Acc) | SST-2 (Acc) | MNLI-m (Acc) | AVERAGE |
|------------|-----------|-----------------|--------------|--------------|--------------|--------------|--------------|
| GPT-2 117M | AdamW | 70.35 | 74.69 | 82.35 | 89.33 | 79.57 | 79.26 |
| | Adafactor | 72.57 | 75.55 | 79.41 | 89.33 | 80.13 | 79.40 |
| | CAME | 70.60 | 69.31 | 64.95 | 82.22 | 76.37 | 72.69 |
| | Adapprox | 72.89 | 75.83 | 80.63 | 90.94 | 80.15 | 80.09 |
| GPT-2 345M | AdamW | 75.06 | 79.39 | 82.84 | 91.17 | 82.33 | 82.16 |
| | Adafactor | 76.23 | 78.90 | 83.33 | 91.06 | 82.62 | 82.43 |
| | CAME | 75.50 | 69.22 | 71.81 | 82.22 | 81.72 | 76.09 |
| | Adapprox | 76.68 | 79.00 | 83.33 | 91.17 | 82.66 | 82.57 |

performance (see Appendix C). Consequently, we recommend retaining the first moment unless memory constraints are extremely prohibitive. Looking towards future research, investigating techniques to compress the first moment could be a promising direction. Furthermore, it is crucial to note that our approach is compatible with other memory optimization techniques such as quantization and recomputation. This compatibility opens the door for potential synergistic enhancements in optimizer design.

6. Conclusion

In this paper, we introduce Adapprox, an innovative optimizer designed to address the memory consumption challenges in training large-scale models. By applying random-

ized low-rank matrix approximation to the second moment of Adam, Adapprox achieves significant memory reduction with minimal impact on model accuracy. This solution is further optimized with an adaptive rank selection mechanism and an optional cosine similarity guidance strategy, enhancing both stability and convergence speed. Our empirical evaluations, encompassing GPT-2 117M and 345M models and their downstream tasks, demonstrate Adapprox’s efficacy. It delivers considerable memory savings, ranging from 33.8% to 49.9% over AdamW with the first moment intact, and between 83.8% to 99.9% when the first moment is excluded. Despite a slight trade-off in memory efficiency, Adapprox outperforms competitors like Adafactor and CAME across several key metrics, including validation loss and perplexity in pretraining, and F1 score and accuracy

in downstream tasks. These results establish Adapprox as a balanced approach for memory-efficient training, effectively harmonizing efficiency with minimal accuracy trade-offs.

Impact Statements

This paper presents work whose goal is to advance the field of Machine Learning. There are many potential societal consequences of our work, none which we feel must be specifically highlighted here.

References

- Anil, R., Gupta, V., Koren, T., and Singer, Y. Memory efficient adaptive optimization. *Advances in Neural Information Processing Systems*, 32, 2019.
- Batselier, K., Yu, W., Daniel, L., and Wong, N. Computing low-rank approximations of large-scale matrices with the tensor network randomized svd. *SIAM Journal on Matrix Analysis and Applications*, 39(3):1221–1244, 2018.
- Brown, T., Mann, B., Ryder, N., Subbiah, M., Kaplan, J. D., Dhariwal, P., Neelakantan, A., Shyam, P., Sastry, G., Askell, A., et al. Language models are few-shot learners. *Advances in neural information processing systems*, 33: 1877–1901, 2020.
- Chen, Y., Guo, Y., Wang, Y., Wang, D., Peng, C., and He, G. Denoising of hyperspectral images using nonconvex low rank matrix approximation. *IEEE Transactions on Geoscience and Remote Sensing*, 55(9):5366–5380, 2017.
- Dolan, B. and Brockett, C. Automatically constructing a corpus of sentential paraphrases. In *Third International Workshop on Paraphrasing (IWP2005)*, 2005.
- Duchi, J., Hazan, E., and Singer, Y. Adaptive subgradient methods for online learning and stochastic optimization. *Journal of machine learning research*, 12(7), 2011.
- Gao, L., Biderman, S., Black, S., Golding, L., Hoppe, T., Foster, C., Phang, J., He, H., Thite, A., Nabeshima, N., et al. The pile: An 800gb dataset of diverse text for language modeling. *arXiv preprint arXiv:2101.00027*, 2020.
- Golub, G. H. and Van Loan, C. F. *Matrix computations*. JHU press, 2013.
- Guo, Q., Gao, S., Zhang, X., Yin, Y., and Zhang, C. Patch-based image inpainting via two-stage low rank approximation. *IEEE transactions on visualization and computer graphics*, 24(6):2023–2036, 2017.
- Haeffele, B., Young, E., and Vidal, R. Structured low-rank matrix factorization: Optimality, algorithm, and applications to image processing. In *International conference on machine learning*, pp. 2007–2015. PMLR, 2014.
- Halko, N., Martinsson, P.-G., and Tropp, J. A. Finding structure with randomness: Probabilistic algorithms for constructing approximate matrix decompositions. *SIAM review*, 53(2):217–288, 2011.
- Kingma, D. P. and Ba, J. Adam: A method for stochastic optimization. *arXiv preprint arXiv:1412.6980*, 2014.
- Krizhevsky, A., Sutskever, I., and Hinton, G. E. Imagenet classification with deep convolutional neural networks. *Communications of the ACM*, 60(6):84–90, 2017.
- Kudo, T. and Richardson, J. Sentencepiece: A simple and language independent subword tokenizer and detokenizer for neural text processing. *arXiv preprint arXiv:1808.06226*, 2018.
- Lee, D. D. and Seung, H. S. Learning the parts of objects by non-negative matrix factorization. *Nature*, 401(6755): 788–791, 1999.
- Li, B., Chen, J., and Zhu, J. Memory efficient optimizers with 4-bit states. *arXiv preprint arXiv:2309.01507*, 2023.
- Li, D., Chen, C., Lv, Q., Yan, J., Shang, L., and Chu, S. Low-rank matrix approximation with stability. In *International Conference on Machine Learning*, pp. 295–303. PMLR, 2016.
- Li, M., Bi, W., Kwok, J. T., and Lu, B.-L. Large-scale nystrom kernel matrix approximation using randomized svd. *IEEE transactions on neural networks and learning systems*, 26(1):152–164, 2014.
- Liberty, E., Woolfe, F., Martinsson, P.-G., Rokhlin, V., and Tygert, M. Randomized algorithms for the low-rank approximation of matrices. *Proceedings of the National Academy of Sciences*, 104(51):20167–20172, 2007.
- Loshchilov, I. and Hutter, F. Decoupled weight decay regularization. In *International Conference on Learning Representations*, 2018.
- Luo, Y., Ren, X., Zheng, Z., Jiang, Z., Jiang, X., and You, Y. Came: Confidence-guided adaptive memory efficient optimization. In *Proceedings of the 61st Annual Meeting of the Association for Computational Linguistics (Volume 1: Long Papers)*, pp. 4442–4453, 2023.
- Nakatsukasa, Y. Fast and stable randomized low-rank matrix approximation. *arXiv preprint arXiv:2009.11392*, 2020.
- Papailiopoulos, D., Dimakis, A., and Korokythakis, S. Sparse pca through low-rank approximations. In *International Conference on Machine Learning*, pp. 747–755. PMLR, 2013.

- Paszke, A., Gross, S., Massa, F., Lerer, A., Bradbury, J., Chanan, G., Killeen, T., Lin, Z., Gimelshein, N., Antiga, L., et al. Pytorch: An imperative style, high-performance deep learning library. In *Advances in Neural Information Processing Systems*, volume 32, pp. 8024–8035, 2019.
- Paterek, A. Improving regularized singular value decomposition for collaborative filtering. In *Proceedings of KDD cup and workshop*, volume 2007, pp. 5–8, 2007.
- Radford, A., Wu, J., Child, R., Luan, D., Amodei, D., Sutskever, I., et al. Language models are unsupervised multitask learners. *OpenAI blog*, 1(8):9, 2019.
- Rajpurkar, P., Zhang, J., Lopyrev, K., and Liang, P. Squad: 100,000+ questions for machine comprehension of text. *arXiv preprint arXiv:1606.05250*, 2016.
- Rokhlin, V., Szlam, A., and Tygert, M. A randomized algorithm for principal component analysis. *SIAM Journal on Matrix Analysis and Applications*, 31(3):1100–1124, 2010.
- Shazeer, N. and Stern, M. Adafactor: Adaptive learning rates with sublinear memory cost. In *International Conference on Machine Learning*, pp. 4596–4604. PMLR, 2018.
- Shen, H. and Huang, J. Z. Sparse principal component analysis via regularized low rank matrix approximation. *Journal of multivariate analysis*, 99(6):1015–1034, 2008.
- Shoeybi, M., Patwary, M., Puri, R., LeGresley, P., Casper, J., and Catanzaro, B. Megatron-lm: Training multi-billion parameter language models using model parallelism, 2019.
- Socher, R., Perelygin, A., Wu, J., Chuang, J., Manning, C. D., Ng, A. Y., and Potts, C. Recursive deep models for semantic compositionality over a sentiment treebank. In *Proceedings of the 2013 conference on empirical methods in natural language processing*, pp. 1631–1642, 2013.
- Steiner, B., Elhoushi, M., Kahn, J., and Hegarty, J. Model: memory optimizations for deep learning. In *International Conference on Machine Learning*, pp. 32618–32632. PMLR, 2023.
- Warstadt, A., Singh, A., and Bowman, S. R. Neural network acceptability judgments. *arXiv preprint arXiv:1805.12471*, 2018.
- Williams, A., Nangia, N., and Bowman, S. R. A broad-coverage challenge corpus for sentence understanding through inference. *arXiv preprint arXiv:1704.05426*, 2017.

A. Ablation Experiment on Clipping Mechanism

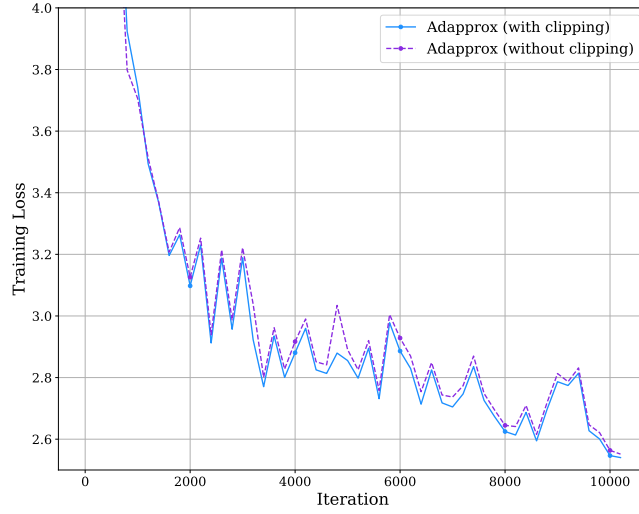


Figure 4. Comparative analysis of training loss for the GPT-2 345M model utilizing Adapprox with and without the clipping mechanism.

Figure 4 provides a comparative analysis of training loss convergence for the GPT-2 345M model utilizing Adapprox with and without the implementation of the clipping mechanism. The results indicate that the inclusion of a clipping mechanism enhances Adapprox’s performance, resulting in lower training losses at equivalent iterations.

B. Learning Rate Sensitivity Analysis

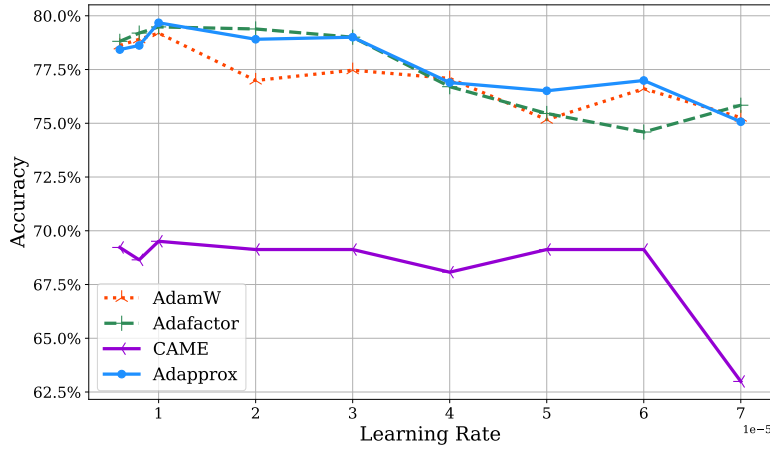


Figure 5. Accuracy of the AdamW-pretrained GPT-2 345M model fine-tuned with compared optimizers on the CoLA task across different learning rates.

In our experiments, Adapprox’s performance demonstrates stability across a range of learning rates. This is illustrated in Figure 5, which compares the accuracy of various optimizers in fine-tuning the AdamW-pretrained GPT-2 345M model on the CoLA task under different learning rate conditions. Notably, Adapprox shows minimal fluctuations, underlining its enhanced stability and lower sensitivity to changes in learning rates.

C. First Moment Efficacy Analysis

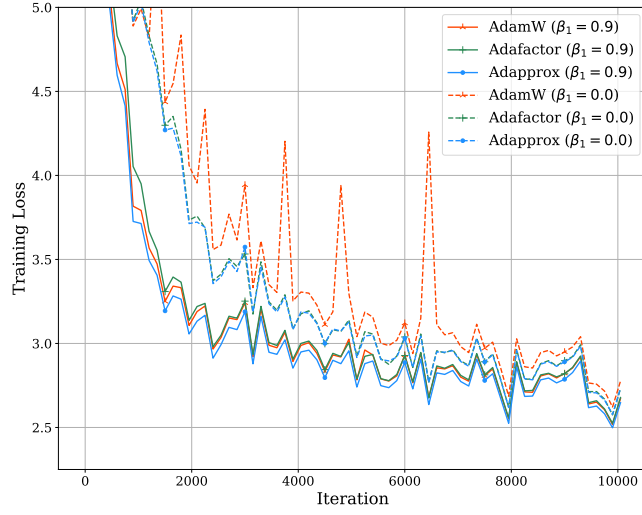


Figure 6. Training loss vs. iteration for AdamW, Adafactor, and Adapprox optimizers, comparing scenarios with and without the first moment.

Figure 6 demonstrates that incorporating the first moment significantly accelerates the convergence process, evidenced by achieving lower training losses at the same iteration, for each optimizer examined, including AdamW, Adafactor, and Adapprox. CAME is omitted from this analysis due to its incompatibility with $\beta_1 = 0$. Furthermore, while AdamW exhibits instability without the first moment, Adafactor and Adapprox mitigate this through the use of a clipping mechanism, effectively reducing large, unexpected updates and enhancing stability.